ORIGINAL PAPER

Synthetic access to new porphyrinoids from 2-nitro-5,10,15,20-tetraphenylporphyrin and an arylacetonitrile

Ouafa Amiri[1,2] · Nuno M. M. Moura[2] (iD) · Maria A. F. Faustino[2] · José A. S. Cavaleiro[2] · El Mostapha Rakib[1] ·
Maria G. P. M. S. Neves[2]

Abstract
In this work, the reactivity of 2-nitro-5,10,15,20-tetraphenylporphyrin with 2-(4-nitrophenyl)acetonitrile in the presence of KOH as base was studied. Under these conditions, three new compounds were isolated: a β-di-substituted derivative, as the major compound, accompanied by two minor products, a π-extended and a β-isoxazoline-fused derivative, all in acceptable yields. A preliminary study was also performed in the presence of K_2CO_3. It allowed the isolation of a cyclopropyl-annulated chlorin in very good yield. All the obtained products were photochemically and photophysically characterized, some of them showing promising properties to be used as photosensitizers in photodynamic processes.

Graphical abstract
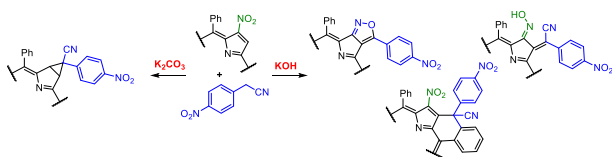
✉ Nuno M. M. Moura
   nmoura@ua.pt

   Maria A. F. Faustino
   faustino@ua.pt

   El Mostapha Rakib
   e.rakib@usms.ma

   Maria G. P. M. S. Neves
   gneves@ua.pt

1 Laboratoire de Chimie Organique et Analytique, Faculté des Sciences et Techniques, Université Sultan Moulay Slimane, BP 523, 2300 Beni-Mellal, Morocco

2 QOPNA and Department of Chemistry, University of Aveiro, 3810-193 Aveiro, Portugal

Introduction

Porphyrins and analogs are nowadays considered to be promising compounds for applications in a broad spectrum of fields, due to their unique photochemical and photophysical properties [1], namely in solar cells [2–4], catalysis [5–7], photocatalysis [8], electronic devices [9–11], biomimetic models [12], supramolecular chemistry [13], (chemo)sensors [14–16], and medicine [17–21].

When envisaging synthetic and reactivity studies having in mind these potential applications, porphyrins like *meso*-tetraarylporphyrins are considered to be good alternatives to the natural ones due to their easy synthetic accessibility and broad spectrum of functionalization either at *meso* or at *β*-pyrrolic positions [22, 23]. In particular, *β*-nitro-*meso*-tetraarylporphyrins are excellent templates for further functionalization through different types of approaches like reduction, nucleophilic addition, nucleophilic or electrophilic substitutions, and cycloaddition reactions [24].

Considering the functionalization of β-nitroporphyrins mediated by nucleophiles, a literature survey shows that the reaction pathway is strongly dependent on the nucleophile, solvent, temperature, the electronic environment on the porphyrinic core and metal coordination. In fact, it is reported that the reaction with "soft" nucleophiles (e.g., thiolates) leads to products resulting from the attack at the carbon atom containing the nitro group (ipso attack), while with "hard" nucleophiles (e.g., oxyanions), the attack occurs preferentially at the β-pyrrolic position adjacent to the nitro group (α-atack) [24–26].

In particular, the reaction of metallo complexes of β-nitro-*meso*-tetraarylporphyrin (β-NO$_2$TPP) with α-isocyanoacetic ester (CNCH$_2$CO$_2$Et) as the nucleophile precursor was reported by Smith et al. in 1996 as a pathway to β-fused pyrroloporphyrins and cyclopropyl-annulated chlorins [27]. In these studies, the authors found that the nickel(II) complex of β-NO$_2$TPP reacts with α-isocyanoacetic esters in the presence of DBU affording β-fused pyrroloporphyrins (the Barton-Zard condensation) while the corresponding zinc(II) complex affords cyclopropanochlorins [28].

Following our interest on the *beta* functionalization of porphyrins via the nitro group, and knowing that the reaction pathway is strongly dependent on the nucleophile, porphyrin core, and experimental conditions, we have undertaken a study involving the reaction of 2-(4-nitrophenyl)acetonitrile as the nucleophile precursor with 2-nitro-5,10,15,20-tetraphenylporphyrin (**1**) as a free base. New products with promising optical features have been isolated. Particular attention was then given to their photophysical features, mainly their ability to generate singlet oxygen (^{1}O$_2$). This is an important requirement for any porphyrin-based photosensitizer (PS) to be used in photodynamic therapy (PDT) of cancer cells [29–33] and in photodynamic inactivation of microorganisms (PDI) [34–39]. The ability of these derivatives to generate cytotoxic reactive oxygen species (ROS), mainly singlet oxygen, after being activated by light is of prominent importance [40, 41]. These reactive oxygen species are the species involved in the biological damages and cell death; their formation is dependent on the efficient conversion of the PS-excited singlet state into the triplet state. The photosensitizer in its triplet state interacts with molecular oxygen (^{3}O$_2$), (mechanism type II), generating ^{1}O$_2$ or takes part in electronic transferences with the surrounding substrates (mechanism type I), generating oxygen radical species [40–43].

Results and discussion

The starting porphyrin, 2-nitro-5,10,15,20-tetraphenylporphyrin (β-NO$_2$TPP, **1**), was prepared by nitration of 5,10,15,20-tetraphenylporphyrin (TPP) using copper

nitrate, acetic acid, and acetic anhydride, followed by demetallation according to well-established procedures [44, 45].

The reactions involving **1** and 2-(4-nitrophenyl)acetonitrile were performed in the presence of KOH (10 equiv.) in THF at reflux. After 1 h of reaction, TLC control showed the total consumption of the starting porphyrin **1** and the formation of three main new products. The results obtained are summarized in Scheme 1. After the work-up and purification by column chromatography, it was possible to identify by a detailed spectroscopic analysis (vide infra) the structure of the three main products, the less abundant ones as being **2** (26% yield, higher R_f) and **3** (18% yield, intermediate R_f), and the major fraction as **4** (47% yield, smaller R_f).

Preliminary studies have also been carried out using K$_2$CO$_3$ as base. The reaction between 2-nitro-5,10,15,20-tetraphenylporphyrin and 2-(4-nitrophenyl)acetonitrile was carried out under the previous experimental conditions but using that base (10 equiv); TLC analysis revealed that after 3 h of reaction, there was formation of a major product. After the work-up and purification, the product was isolated in 86% yield; its spectroscopic data are consistent with the structure of the cyclopropyl-annulated chlorin **5** (Fig. 1).

Mechanistic considerations

A probable pathway leading to the formation of the compounds shown in Scheme 1 is outlined in Scheme 2. The structure of the compounds obtained suggests that in all cases, the initial attack of the carbanion occurs at the β-pyrrolic position adjacent to the nitro group leading to species **A**. This species in the presence of KOH can follow two different ways: (1) a prototropic rearrangement followed by dehydration leads to the formation of compound **4**. Then, this compound after an intramolecular cyclization followed by loss of HCN can justify the formation of β-fused oxazoline **2**. This proposal was corroborated by the obtention of compound **2** after heating compound **4** in THF for 2.5 h in the presence of KOH.

Alternatively, (2) the aerial oxidation of intermediate **A** followed by an intramolecular cyclization involving the acrylonitrile moiety and the *meso*-phenyl ring adjacent at intermediate **C** leads to **D** that after oxidation can give rise to compound **3** (Scheme 2). This type of intra-cyclization is probably favored by the conjugation of the electron-withdrawing NO$_2$H group with the acrylonitrile unit [46–48].
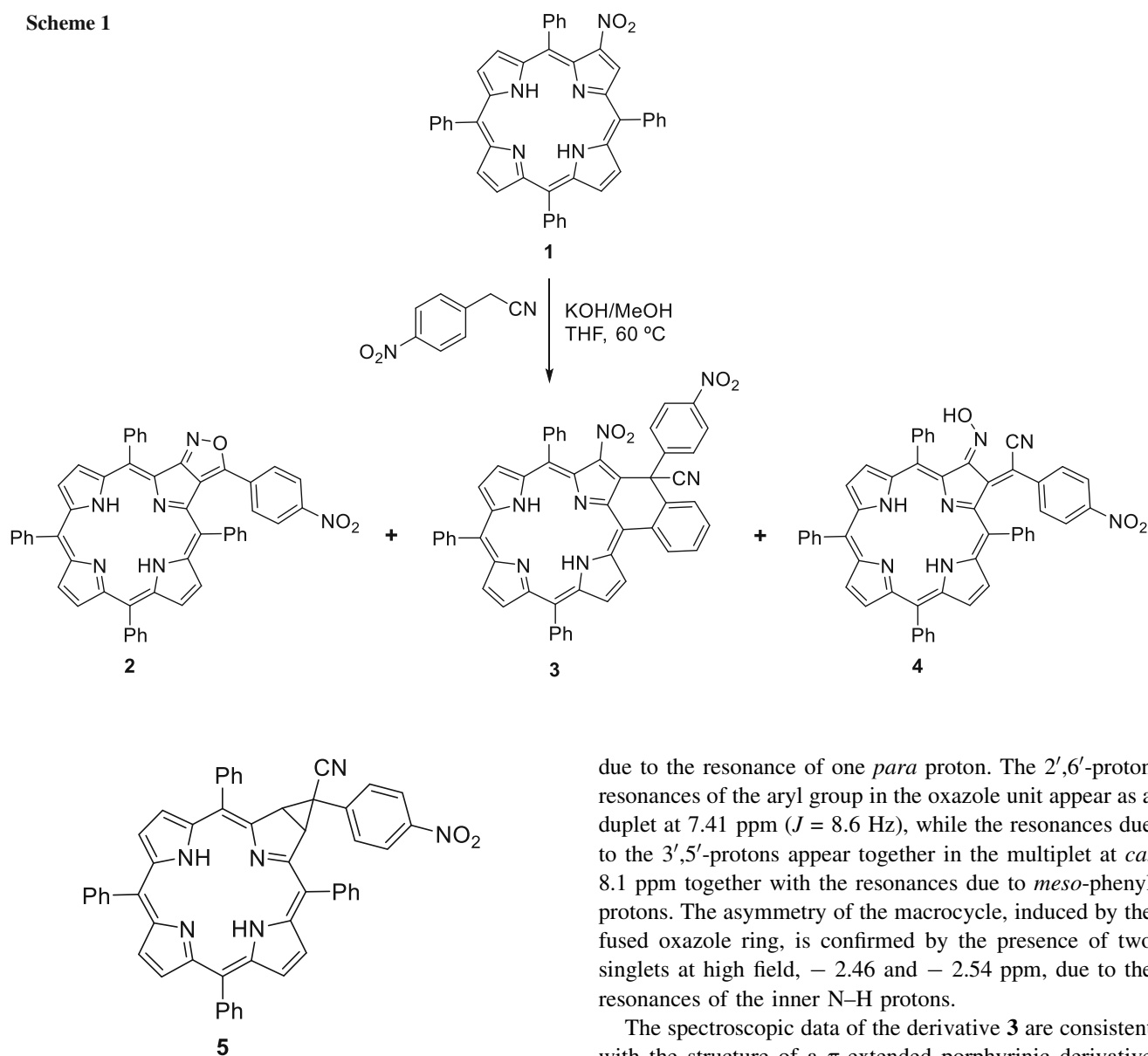
Scheme 1

1

+CN / KOH/MeOH THF, 60 °C

O_2N

2   +   **3**   +   **4**

5

Fig. 1 Structure of cyclopropyl-annulated chlorin **5**

Structural characterization

The structural elucidation of all compounds involved the use of 1D (^{1}H and ^{13}C spectra) and 2D [(^{1}H,^{1}H) COSY, (^{1}H,^{13}C) HSQC, and (^{1}H,^{13}C) HMBC] NMR techniques and of high-resolution mass spectrometry (HRMS-ESI) (see "Experimental" section and SI).

The ^{1}H NMR of compound **2** shows the resonances of only six β-pyrrolic in the range from $\delta = 8.5$ to 8.9 ppm, consistent with a substituted porphyrin with a β,β'-fused ring. The mass spectrum shows a peak at $m/z = 777.3$ corresponding to the (M+H)$^+$ ion (see SI, Fig S1–S7). The protons of the *meso*-phenyl groups appear as multiplets between ca. 7.3 and 8.2 ppm and one triplet at 7.13 ppm

due to the resonance of one *para* proton. The 2′,6′-proton resonances of the aryl group in the oxazole unit appear as a duplet at 7.41 ppm ($J = 8.6$ Hz), while the resonances due to the 3′,5′-protons appear together in the multiplet at *ca.* 8.1 ppm together with the resonances due to *meso*-phenyl protons. The asymmetry of the macrocycle, induced by the fused oxazole ring, is confirmed by the presence of two singlets at high field, $- 2.46$ and $- 2.54$ ppm, due to the resonances of the inner N–H protons.

The spectroscopic data of the derivative **3** are consistent with the structure of a π-extended porphyrinic derivative (Fig. S8–S14 of ESI). In the ^{1}H NMR spectrum, the signals due to the resonances of the *meso*-phenyl protons appear at *ca.* 7.5–8.3 ppm. In this case, the resonances of the N–H protons from the inner core appear as singlet at $- 1.68$ ppm suggesting a decrease in the porphyrin ring current when compared with compound **2**. The mass spectrum of this compound is also in accordance with the proposed structure, presenting a peak at $m/z = 818.3$, corresponding to the (M+H)$^+$ ion.

The structure of derivative **4** was established by considering its mass spectrum, which shows the (M+H)$^+$ ion at $m/z = 805.3$ and NMR studies (Fig. S15–S21 of ESI). The ^{1}H NMR of compound **4** shows the resonances of only six β-pyrrolic in the range *ca.* 8.8–8.3 ppm. The resonances of the protons of three of the *meso*-phenyl groups appear as two multiplets between *ca.* 7.8 and 8.2 ppm and one duplet

Scheme 2
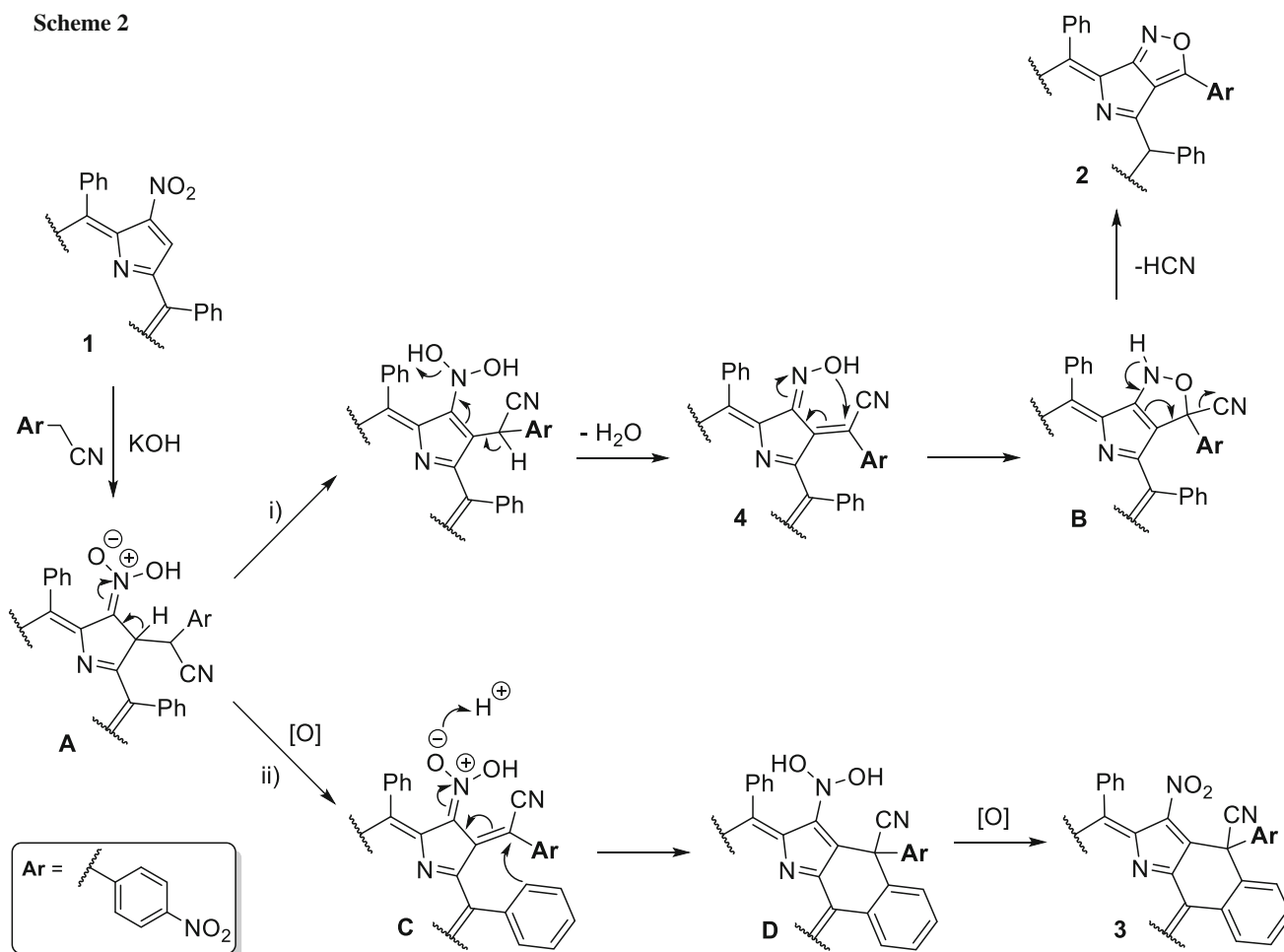
at 8.1 ppm (J = 7.9 Hz), while the signals due to the resonances of one *meso*-phenyl ring are significantly protected appearing at *ca.* 7.3 and 7.6 ppm. The resonances of the *p*-nitrophenyl ring of the acetonitrile moiety appear as two duplets at 6.9 and 7.8 ppm (J = 8.5 Hz). Once again, a decrease in the porphyrin ring current is patent by the appearance of the inner N–H resonances as two singlets at − 1.90 and − 1.97 ppm.

Finally, for compound **5**, its mass spectrum showed a base peak at *m/z* = 775.3 corresponding to the expected $(M+H)^+$ ion, and the ^1H NMR spectrum is in accordance with a symmetric molecule as it is shown by the resonances of H-2 and H-3, from the reduced *β*-pyrrolic positions, and of the N–H protons as singlets, respectively, at 4.7 and − 1.9 ppm (see SI, Fig S22–S29).

Photophysical characterization

The absorption, emission and excitation spectra of the β-functionalized porphyrins **2–5** were recorded in DMF

solutions (10^{-6} M) at 298 K. All the results are summarized in Table 1 and Fig. 2.

The absorption spectrum of derivative **2** in DMF clearly shows the typical features of a free-base *meso*-tetraphenylporphyrin due to π–π* transitions [49, 50]. In this etio-type spectrum, the highly intense Soret band appears centered at 425 nm and the less intense and well-defined four *Q* bands appear between 522 and 648 nm. In the absorption spectra of derivative **3,** the Soret band is significantly broadened and red-shifted to 429 nm with a shoulder band at *ca.* 450 nm. The *Q* bands of this porphyrin are also significantly red-shifted and much enhanced, showing three bands at 626, 676, and 758 nm. Presumably, this behavior observed for compound **3** may be related with a non-planar distortion of the porphyrin macrocycle due to the fusion between the *meso*-phenyl ring and the side chain at the *β*-pyrrolic position (Fig. 2a).

Compound **4** shows a UV–Vis spectrum with a significant red-shifted Soret band (446 nm) and four *Q* bands centered between 548 and 689 nm with relative intensity of IV = I > II > III. Compound **5** shows a similar absorption

Table 1 Photophysical data of compounds **2–5** in DMF at 298 K

Compound	λ_{max}/nm:log ε	λ_{em}/nm	Stoke's shift (nm)	Φ_{Flu}
2	425:5.41	653, 724	5	0.14
	522:4.30			
	553:3.87			
	595:3.90			
	648:3.52			
3	429:5.38	–	–	–
	506:4.60			
	626:4.65			
	676:4.67			
	758:4.68			
4	446:4.92	–	–	–
	548:3.78			
	589:3.60			
	630:3.21			
	689:3.78			
5	427:5.26	654, 723	4	0.14
	519:4.24			
	549:3.93			
	596:3.81			
	650:4.24			

spectrum; however, it is blue-shifted *ca.* 20 nm when compared with the spectrum of compound **4** (Fig. 2a).

The steady-state fluorescence emission spectra of **2** and **5** were measured in DMF, after their excitation at *ca.* 550 nm (see Fig. 2b). The porphyrinic derivatives **2** and **5** present the typical features of *meso*-tetraarylporphyrins [51] with two bands centered at *ca.* 655 and at 725 nm, where the first vibrational mode of the fluorescence is much more pronounced than the second one. The emission bands could be assigned to $Q_x(0–0)$ and $Q_x(0–1)$ transitions, typical of free-base porphyrins due to a nearly unchanged vibronic state upon excitation [52].

Fluorescence quantum yields (Φ_{Flu}) of the studied compounds **2** and **5** were determined by the internal reference method in DMF using TPP ($\Phi_{Flu} = 0.11$) as a standard in the S_1 state (Table 1) [53, 54]. The values of Φ_{Flu} for derivatives **2** and **5** are slightly higher ($\Phi_{Flu} = 0.14$) than those of the reference TPP. However, it is worth mentioning that the fluorescence quantum yield determined for compounds **3** and **4**, without fused rings at beta positions, is lower than 1%, relatively to the reference TPP, indicating a quenching of the porphyrin-excited singlet state. This quenching observed is probably due to the presence of electron-withdrawing groups in the beta pyrrolic position for both compounds, and a distortion induced by the fused ring in compound **3**.

These compounds show, in general, low Stokes shifts (≈ 5 nm), indicating that in the studied compounds the spectroscopic energies are similar to the relaxed energies of the lowest singlet excited state S1, which suggests the occurrence of a minor geometric relaxation in the first excited state.

Singlet oxygen generation

It is well established that the potentiality of a porphyrin to be used in photodynamic processes, namely as a photosensitizer in photodynamic therapy, is strongly related with its ability to generate ROS, mainly singlet oxygen ($^1O_2$). The ability to produce $^1O_2$ of all porphyrins was qualitatively estimated using 1,3-diphenylisobenzofuran (DPiBF) as the $^1O_2$ scavenger [55]. The yellow DPiBF (with a maximum wavelength at 415 nm) reacts with $^1O_2$ generated by the combined action of light, porphyrin and dissolved oxygen in a [4 + 2] cycloaddition affording the colorless *o*-dibenzoylbenzene. The decay of DPiBF absorption band at 415 nm allows the evaluation of the ability of each porphyrin to generate $^1O_2$. 5,10,15,20-tetraphenylporphyrin (TPP) was used as the reference, which is known to be a good oxygen generator [56].

The $^1O_2$ generation assessment results obtained with the porphyrins **2–5** are represented in Fig. 3 and they confirm that all the studied porphyrins are able to induce a decrease in the DPiBF absorption. It is worth to refer that the absorbance of DPiBF when irradiated under the same conditions, but without the presence of the studied porphyrin derivatives, remains almost unchanged ($\approx 2\%$) and the DPiBF photodecomposition is enhanced, in particular, in the presence of the compound **5** (Fig. 3).

When compared with TPP and under the same irradiation conditions, the efficiency of the derivatives **2–4** is significantly lower, with a variation in the range 65–30%. A different situation was observed with derivative **5** where the ability to photo-oxidize DPiBF is almost two times higher than the one observed with TPP. These data show that the structure of each derivative in conjugation with its photophysical properties are key features in its ability to generate $^1O_2$. The ability to generate $^1O_2$, namely for compound **5**, after being exposed to light in the presence of dissolved oxygen, allowed to envisage their potentiality to be used as PSs in photodynamic processes.

Conclusion

In summary, new porphyrinoids were obtained from the reaction of 2-nitro-5,10,15,20-tetraphenylporphyrin with 2-(4-nitrophenyl)acetonitrile. Such products are the disubstituted derivative **4** (the major compound) and two
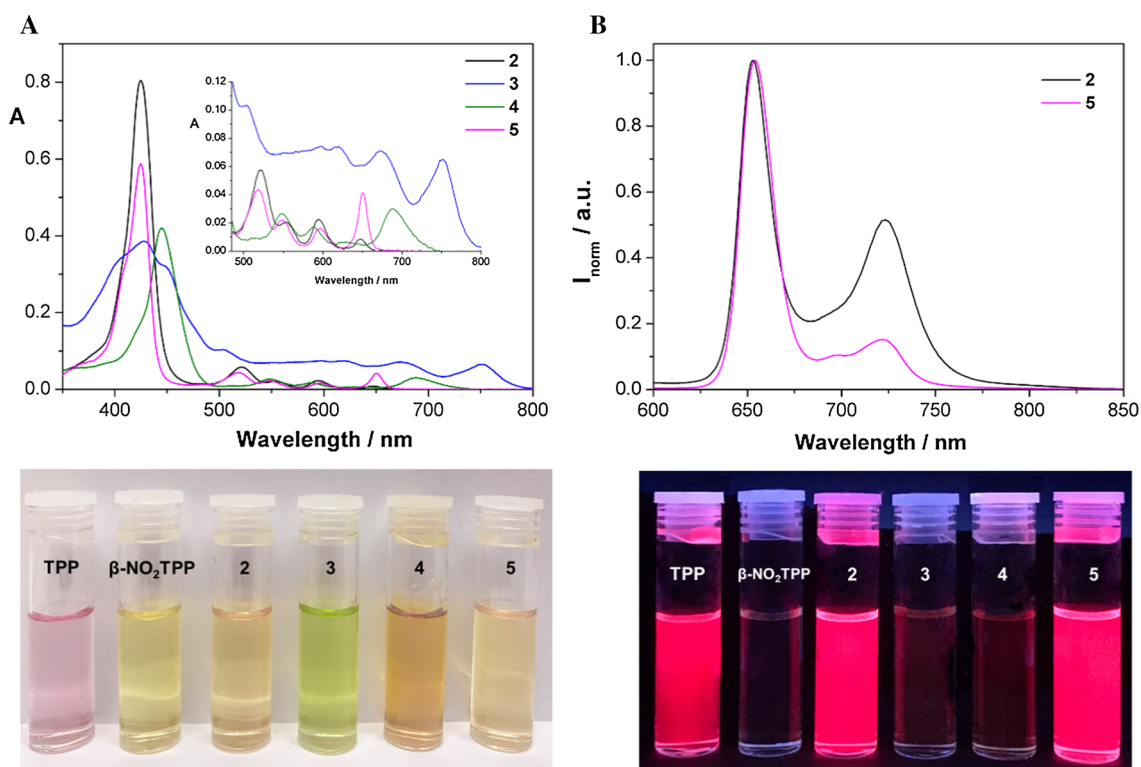
Fig. 2 Top: Absorption (**a**) and normalized emission (**b**) of compounds **2–5** in DMF at room temperature. ([**2**] = [**3**] = [**4**] = [**5**] = 2.5 × 10^{-6} M; λ_{exc2}= 553 and λ_{exc5}=549 nm). The inset in **A** highlights the Q bands region. Bottom:

physical appearance of a solution of TPP, β-NO$_2$TPP, and compounds **2-5** in DMF at 2.5 × 10^{-6} M under visible light (left) and after excitation at 365 nm using a fluorescent lamp (right)
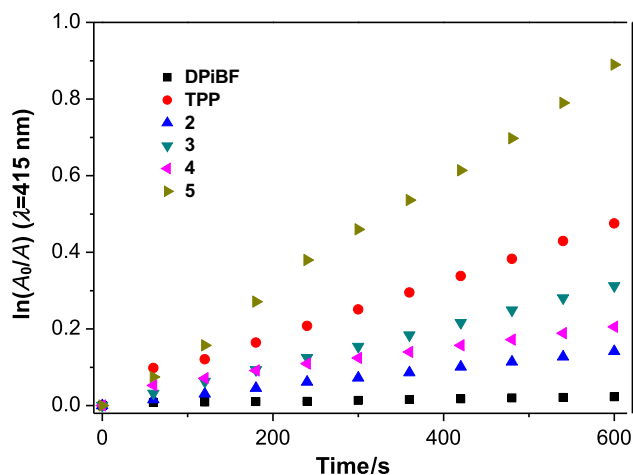

Fig. 3 Time-dependent photodecomposition of DPiBF (50 μM) alone and in the presence of derivatives **2–5** and TPP at 0.5 (μM) in DMF upon irradiation with red light (630 ± 20 nm) with an irradiance of 9.0 mW cm^{-2}

minor ones (the π-extend derivative **3** and the β-isoxazoline-fused derivative **2**). We also obtained the chlorin-type derivative **5**.

The synthesized porphyrinoids not only possess good absorbances in the visible region of the electromagnetic spectrum (400–700 nm) but also are good singlet oxygen generators which make them interesting compounds for the use as photosensitizers in photodynamic treatments.

Experimental

^{1}H and ^{13}C solution NMR spectra were recorded on Bruker Avance 300 (300.13 and 75.47 MHz, respectively) and Avance 500 (500.13 and 125.76 MHz, respectively) spectrometers. CDCl$_3$ was used as solvent and tetramethylsilane (TMS) as the internal reference; the chemical shifts are expressed in δ (ppm) and the coupling constants (J) in Hertz (Hz). Unequivocal ^{1}H assignments were made using 2D COSY (^{1}H/^{1}H), while ^{13}C assignments were made based on 2D HSQC (^{1}H/^{13}C) and HMBC (delay for long-range $J_{\text{C/H}}$ couplings were optimized for 7 Hz) experiments. Mass spectra were recorded using a MALDI TOF/TOF 4800 Analyzer, Applied Biosystems MDS Sciex, with CHCl$_3$ as solvent and without matrix. Mass spectra HRMS were recorded on an APEXQe FT-ICR (Bruker Daltonics, Billerica, MA) mass spectrometer using CHCl$_3$ as solvent, in m/z (rel.%). Preparative thin-layer chromatography was carried out on 20 × 20 cm glass plates coated with silica gel (0.5 mm thick). Column chromatography was carried

out using silica gel (Merck, 35–70 mesh). Analytical TLC was carried out on precoated sheets with silica gel (Merck 60, 0.2 mm thick). All the chemicals were used as supplied. Solvents were purified or dried according to the literature procedures [57].

Synthesis of the precursor 2-nitro-5,10,15,20-tetraphenylporphyrin (1)

The 2-nitro-5,10,15,20-tetraphenylporphyrin (**1**) was prepared from 5,10,15,20-tetraphenylporphyrin by treatment with copper nitrate in the presence of acetic anhydride, followed by demetallation of the 2-nitroporphyrinatocopper(II) under acidic conditions as it is described in the literature [44, 45]. The structure of the synthesized compound was confirmed by the ^{1}H NMR and mass spectroscopic data.

Synthesis of compounds 2-4: general procedure

To a solution of 30.0 mg of 2-nitro-5,10,15,20-tetraphenylporphyrin (**1**, 4.6×10^{-5} mol) and 7.4 mg 2-(4-nitrophenyl)acetonitrile (1.0 equiv., 4.6×10^{-5} mol) in 1.5 cm^3 THF was added 0.75 cm^3 of a methanolic solution of potassium hydroxide (25.8 mg, 10.0 equiv., 4.6×10^{-4} mol). The mixture was stirred for 1 h at 65 °C. After cooling, the pH was adjusted to 7 with a 10% HCl aqueous solution; the reaction mixture was washed with water and extracted with dichloromethane. The organic phase was dried (Na$_2$SO$_4$), and the solvent was evaporated under reduced pressure. The crude mixture was submitted to column chromatography (silica gel) using toluene/hexane (1:1) as the eluent. The fractions obtained were fully characterized by NMR, mass, and spectroscopic techniques after crystallization in a CH$_2$Cl$_2$/hexane mixture.

3-(4-Nitrophenyl)-5,10,15,20-tetraphenylisoxazolo[2,3-c]-porphyrin (2, C$_{51}$H$_{32}$N$_6$O$_3$)

Purple solid, 9.3 mg, 26% yield. M.p.: > 300 °C; ^{1}H NMR (500 MHz, CDCl$_3$): δ = 8.89 (1H, d, J = 4.9 Hz, H-β), 8.81–8.76 (2H, m, H-β), 8.68 and 8.66 (2H, AB system, J = 4.9 Hz, H-β), 8.56 (1H, d, J = 5.0 Hz, H-β), 8.21–8.17 (6H, m, H–o-Ph), 8.08–8.06 (4H, m, H–o-Ph and H-3′,5′), 7.87–7.84 (3H, m, H-m,p-Ph), 7.80–7.73 (6H, m, H-m,p-Ph), 7.41 (2H, d, J = 8.6 Hz, H-2′,6′), 7.29–7.27 (2H, m, H-m-Ph), 7.13 (1H, t, J = 7.6 Hz, H-p-Ph), − 2.46 (1H, s, NH), − 2.54 (1H, s, NH) ppm; ^{13}C NMR (125 MHz, CDCl$_3$): δ = 194.5, 159.6, 155.0, 154.6, 147.5, 147.5, 135.0, 134.5, 134.4, 133.1, 129.5, 128.0, 127.8, 126.9, 126.8, 123.0, 116.4, 116.1 ppm; UV–Vis (DMF, c = 2.5×10^{-4} mol dm^{-3}): λ_{max} (ε) = 425 (256,740), 522 (20,002), 553, (7447), 595 (7901), 648 (3275) nm (mol^{-1} dm^3 cm^{-1}); MS (ESI(+), 70 eV): m/z = 777.3 ([M+H]$^+$); HRMS (ESI(+), 70 eV): m/z calculated to C$_{51}$H$_{33}$N$_6$O$_3$ ([M+H]$^+$) 777.2609, found 777.2605

2-Nitro-10,15,20-triphenyl-5′-cyano-5′-(4-nitrophenyl)naphtho[1,2,3-at]porphyrin (3, C$_{52}$H$_{31}$N$_7$O$_4$)

Dark green solid, 6.7 mg, 18% yield. M.p.: > 300 °C; ^{1}H NMR (500 MHz, CDCl$_3$): δ = 9.68 (1H, d, J = 5.0 Hz, H-β), 8.96 (1H, d, J = 5.0 Hz, H-β), 8.78 and 8.76 (2H, AB system, J = 5.0 Hz, H-β), 8.66 and 8.63 (2H, AB system, J = 4.8 Hz, H-β), 8.53 (1H, dd, J = 8.0, 1.0 Hz, H-Ph$_a$), 8.31–8.29 (1H, m, H–o-Ph), 8.23-8.21 (1H, m, H–o-Ph), 8.12–8.03 (5H, m, H–o-Ph, H-3′,5′), 7.95 (1H, d, J = 7.9 Hz, H–o-Ph), 7.89 (1H, dd, J = 8.0, 1.0 Hz, H-Ph$_c$), 7.82–7.69 (12H, m, H-m,p-Ph, H-Ph$_b$ and H-2′,6′), 7.64–7.55 (3H, H-m,p-Ph and H-Ph$_d$), − 1.68 (2H, s, NH) ppm; ^{13}C NMR (125 MHz, CDCl$_3$): δ = 157.1, 147.6, 145.2, 140.9, 140.6, 139.7, 139.5, 139.4, 138.3, 138.2, 135.82, 135.77, 135.65, 134.6, 134.4, 134.1, 130.5, 129.9, 129.2, 129.1, 128.9, 128.6, 128.5, 128.34, 128.26, 128.0, 127.2, 127.1, 124.3, 122.2, 122.0, 121.6, 111.7 ppm; UV–Vis (DMF, c = 2.5×10^{-4} mol dm^{-3}): λ_{max} (ε) = 429 (237,314), 506 (39,913), 626 (44,959), 676 (47,088), 758 (48,028) nm (mol^{-1} dm^3 cm^{-1}); MS (ESI(+), 70 eV): m/z = 818.3 ([M+H]$^+$); HRMS (ESI(+), 70 eV): m/z calculated to C$_{52}$H$_{35}$N$_6$O$_2$ ([M+H]$^+$) 818.2510, found 818.2514.

2-(Hydroximino)-3-[1′-cyano-1′-(4-nitrophenyl)methylene]-5,10,15,20-tetraphenylporphyrin (4, C$_{52}$H$_{33}$N$_7$O$_3$)

Purple solid, 17.2 mg, 47% yield. M.p.: > 300 °C; ^{1}H NMR (500 MHz, CDCl$_3$): δ = 8.76 (1H, d, J = 4.9 Hz, H-β), 8.71 (1H, d, J = 4.9 Hz, H-β), 8.62 (1H, d, J = 4.9 Hz, H-β), 8.58 and 8.57 (2H, AB system, J = 4.9 Hz, H-β), 8.38 (1H, d, J = 4.9 Hz, H-β), 8.20–8.17 (4H, m, H–o-Ph), 8.09 (2H, d, J = 7.9 Hz, H–o-Ph), 7.84 (2H, d, J = 8.5 Hz, H-3′,5′),7.81–7.75 (9H, m, H-m,p-Ph), 7.62 (2H, d, J = 7.4 Hz, H–o-Ph), 7.47–7.44 (1H, m, H-p-Ph), 7.34 (2H, t, J = 7.4 Hz, H-m-Ph), 6.92 (2H, d, J = 8.5 Hz, H-2′,6′), − 1.90 (1H, s, NH), − 1.97 (1H, s, NH) ppm; ^{13}C NMR (125 MHz, CDCl$_3$): δ = 163.9, 160.4, 156.2, 155.2, 147.8, 142.8, 142.6, 141.7, 140.9, 140.2, 140.0, 139.4, 138.2, 137.9, 136.2, 135.7, 134.9, 134.5, 134.1, 133.4, 131.0, 128.8, 128.7, 128.5, 128.3, 128.2, 128.13, 128.05, 127.7, 127.6, 127.5, 127.1, 123.6, 123.1, 122.8, 122.7, 117.3, 115.3 ppm; UV–Vis (DMF, c = 2.5×10^{-4} mol dm^{-3}): λ_{max} (ε) = 446 (83,171), 548 (6017), 589 (3959), 630 (1629), 689 (6065) nm (mol^{-1} dm^3 cm^{-1}); MS (ESI(+), 70 eV): m/z = 805.3 ([M + 2H]$^+$); HRMS (ESI(+), 70 eV): m/z calculated to C$_{52}$H$_{35}$N$_7$O$_3$ ([M + 2H]$^+$); 805.2534, found 805.2549.

1′-Cyano-1′-(4-nitrophenyl)-5,10,15,20-tetraphenyl-2H,3H-cyclopropano[2,3-b]porphyrin (5, C$_{52}$H$_{34}$N$_6$O$_2$)

To a solution of 30.0 mg of 2-nitro-5,10,15,20-tetraphenylporphyrin (**1**, 4.6×10^{-5} mol) and 7.4 mg 2-(4-

nitrophenyl)acetonitrile (1.0 equiv., 4.6×10^{-5} mol) in 1.5 cm^3 of THF was added 0.75 cm^3 of methanolic potassium carbonate (63.6 mg, 10.0 equiv., 4.6×10^{-4} mol). The mixture was stirred for 3 h at 65 °C. After cooling, the pH was adjusted to 7 with a 10% HCl aqueous solution and the reaction mixture was washed with distilled water and extracted with dichloromethane. The organic phase was dried (Na$_2$SO$_4$), and the solvent was evaporated under reduced pressure. The crude mixture was submitted to column chromatography (silica gel) using toluene/hexane (1:1) as the eluent. The fractions obtained were fully characterized by NMR, mass, and spectroscopic techniques after crystallization in a CH$_2$Cl$_2$/hexane mixture. Purple solid, 30.3 mg, 86% yield. M.p.: > 300 °C; ^{1}H NMR (500 MHz, CDCl$_3$): δ = 8.73 (1H, d, J = 4.8 Hz, H-β), 8.52–8.50 (4H, m, H-β), 8.26 (2H, d, J = 8.6 Hz, H-3′,5′), 8.16–8.10 (6H, m, H–o-Ph), 7.99 (2H, d, J = 7.3 Hz, H–o-Ph), 7.78-7.62 (12H, m, H-m,p-Ph), 7.49 (2H, d, J = 8.6 Hz, H-2′,6′), 4.74 (2H, s, H-2 and H-3), − 1.88 (1H, s, NH) ppm; ^{13}C NMR (125 MHz, CDCl$_3$): δ = 156.6, 153.9, 147.5, 142.9, 142.1, 141.8, 139.9, 137.0, 136.2, 134.2, 134.0, 133.8, 133.3, 132.1, 129.0, 128.7, 128.2, 128.1, 128.0, 127.9, 127.3, 126.9, 126.7, 124.9, 124.4, 124.3, 123.6, 116.6, 116.4, 114.2, 48.8 ppm; UV–Vis (DMF, c = 2.5×10^{-4} mol dm^{-3}): λ_{max} (ε) = 427 (182,823), 519 (17,206), 549 (8559), 596 (6458), 650 (17,297) nm (mol^{-1} dm^3 cm^{-1}); MS (ESI(+), 70 eV): m/z = 775.3 ([M+H]$^+$); HRMS (ESI(+), 70 eV): m/z calculated to C$_{52}$H$_{35}$N$_6$O$_2$ ([M+H]$^+$) 775.2816, found 775.2803.

Spectrophotometric and spectrofluorometric measurements

The absorption spectra were recorded on a UV-2501PC Shimadzu spectrophotometer and the fluorescence emission spectra were recorded on a Horiba Jobin–Yvon Fluoromax 3 spectrofluorimeter using DMF as solvent. The linearity of the fluorescence emission versus the concentration was checked in the concentration range used (10^{-4}–10^{-6} M). The studied solutions were prepared by appropriate dilution of the stock solutions up to 10^{-5}–10^{-6} M. All the measurements were performed at 298 K.

Fluorescence quantum yields of all compounds studied (**1-5**) were measured using a solution of 5,10,15,20-tetraphenylporphyrin (TPP) in dimethylformamide (DMF) as standard (Φ_{Flu} = 0.11) [58], and all values were corrected taking into account the solvent refractions index.

Singlet oxygen generation

A stock solution of each porphyrin derivative at 0.1 mM in DMF and a stock solution of 1,3-diphenylisobenzofuran

(DPiBF) at 10 mM in DMF were prepared. Aliquots of 2.5 cm^3 of a solution of each porphyrin (0.5 μM) and DPiBF (50 μM) in DMF were irradiated in a glass cuvette, at room temperature and under gentle magnetic stirring. As the light source, a homemade red LED array was used to prevent the photodegradation of DPiBF. The LED array is composed of a matrix of 5×5 LED that makes a total of 25 light sources with an emission peak at 630 nm and a bandwidth at half maximum of ± 20 nm and an irradiance of 9.0 mW cm^{-2}, measured with an energy power meter Coherent FieldMaxII-Top combined with a Coherent PowerSens PS19Q energy sensor.

The absorption decay of DPiBF at 415 nm was measured at irradiation intervals up to 10 min (600 s). The production of singlet oxygen was evaluated qualitatively through the DPiBF, a singlet oxygen (^{1}O$_2$) quencher, due to the fact that DPiBF decays in a first order manner during continuous irradiation in a photosensitized experiment. The irradiation of the PS in the presence of dissolved oxygen will result in the formation of ^{1}O$_2$, which is trapped by DPiBF resulting in colorless o-dibenzoylbenzene, after the Diels–Alder-like reaction with ^{1}O$_2$.

References

1. Kadish KM, Smith KM, Guilard R (2010) Handbook of Porphyrin Science. World Scientific Publishing Company Co, Singapore
2. Di Carlo G, Biroli AO, Tessore F, Caramori S, Pizzotti M (2018) Coord Chem Rev 358:153
3. Kundu S, Patra A (2017) Chem Rev 117:712
4. Vamsi KN, Suman KJV, Madoori M, Seelam P, Lingamallu G (2017) Chemsuschem 10:4668
5. Nakagaki S, Mantovani K, Sippel Machado G, de Freitas Dias, Castro K, Wypych F (2016) Molecules 21:291
6. Costentin C, Robert M, Savéant J-M (2015) Acc Chem Res 48:2996
7. Pegis ML, Wise CF, Martin DJ, Mayer JM (2018) Chem Rev 118:2340
8. Zhang W, Lai W, Cao R (2017) Chem Rev 117:3717
9. Jurow M, Schuckman AE, Batteas JD, Drain CM (2010) Coord Chem Rev 254:2297
10. Niu T, Li A (2013) J Phys Chem Lett 4:4095
11. Auwärter W, Écija D, Klappenberger F, Barth JV (2015) Nat Chem 7:105
12. Lu H, Kobayashi N (2016) Chem Rev 116:6184
13. Otsuki J (2018) J Mater Chem A 6:6710
14. Paolesse R, Nardis S, Monti D, Stefanelli M, Di Natale C (2017) Chem Rev 117:2517

15. Ding Y, Zhu W-H, Xie Y (2017) Chem Rev 117:2203
16. Figueira F, Rodrigues JMM, Farinha AAS, Cavaleiro JAS, Tomé JPC (2016) J Porphyrins Phthalocyanines 20:950
17. Singh S, Aggarwal A, Bhupathiraju NVSDK, Arianna G, Tiwari K, Drain CM (2015) Chem Rev 115:10261
18. Calvete MJF, Pinto SMA, Pereira MM, Geraldes CFGC (2017) Coord Chem Rev 333:82
19. Zhou Y, Liang X, Dai Z (2016) Nanoscale 8:12394
20. Diogo P, Fernandes C, Caramelo F, Mota M, Miranda IM, Faustino MAF, Neves MGPMS, Uliana MP, Santos JM, Gonçalves T (2017) Front Microbiol 8:498
21. Marciel L, Teles L, Moreira B, Pacheco M, Lourenço LMO, Neves MGPMS, Tomé JPC, Faustino MAF, Almeida A (2017) Future. Med Chem 9:365
22. Cerqueira A, Moura NMM, Serra VIV, Faustino MAF, Tomé AC, Cavaleiro JAS, Neves MGPMS (2017) Molecules 22:1269
23. Cavaleiro JAS, Tomé AC, Neves MGPMS (2010) Meso-tetraarylporphyrin derivatives: New synthetic methodologies. In: Kadish KM, Smith KM, Guilard R (eds) Handbook of porphyrin science. World Scientific Publishing Company Co, Singapore, p 193
24. Serra VIV, Pires SMG, Alonso CMA, Neves MGPMS, Tomé AC, Cavaleiro JAS (2014) Meso-tetraarylporphyrins bearing nitro or amino groups: synthetic strategies and reactivity profiles. In: Paolesse R (ed) Synthesis and modifications of porphyrinoids. Springer, Berlin, p 35
25. Crossley MJ, King LG, Simpson JL (1997) J Chem Soc Perkin Trans 1 3087 and references herein cited
26. Jaquinod L (2000) Functionalization of 5,10,15,20-tetra-substituted porphyrins. In: Kadish KM, Smith KM, Guilard R (eds) The porphyrin handbook. Academic, San Diego, p 212
27. Jaquinod L, Gros C, Olmstead MM, Antolovich M, Smith KM (1996) Chem Commun 1475
28. Jaquinod L, Gros C, Khoury RG, Smith KM (1996) Chem Commun 2581
29. Luo D, Carter KA, Miranda D, Lovell JF (2017) Adv Sci 4:1600106
30. Ethirajan M, Chen Y, Joshi P, Pandey RK (2011) Chem Soc Rev 40:340
31. Abrahamse H, Hamblin MR (2016) Biochem J 473:347
32. Josefsen LB, Boyle RW (2012) Theranostics 2:916
33. Gomes ATPC, Neves MGPMS, Cavaleiro JAS (2018) An Acad Bras Ciênc 90:993
34. Alves E, Faustino MAF, Neves MGPMS, Cunha Â, Nadais H, Almeida A (2015) J Photochem Photobiol C 22:34
35. Tim M (2015) J Photochem Photobiol B 150:2
36. Rosa LP, Silva FC (2014) J Med Microb Diagn 3:158
37. Sperandio FF, Ying-Ying H, Hamblin MR (2013) Recent Pat Anti-Infect Drug Discov 8:108
38. Adolfo VDM, Haynes MH, Ball AB, Tianhong D, Christos A, Kelso MJ, Hamblin MR, Tegos GP (2012) Photochem Photobiol 88:499
39. Wainwright M, Maisch T, Nonell S, Plaetzer K, Almeida A, Tegos GP, Hamblin MR (2017) Lancet Infect Dis 17:e49
40. Marko AJ, Patel NJ, Joshi P, Missert JR, Pandey RK (2016) In: Pandey RK, Kessel D, Dougherty TJ (eds) Handbook of photodynamic therapy—updates on recent applications of porphyrin-based compounds. World Scientific Publishing Co, Singapore, p 3
41. van Straten D, Mashayekhi V, de Bruijn HS, Oliveira S, Robinson DJ (2017) Cancers 9:54
42. Baptista MS, Cadet J, Di Mascio P, Ghogare AA, Greer A, Hamblin MR, Lorente G, Nunez SC, Ribeiro MS, Thomas AH, Vignoni M, Yoshimura TM (2017) Photochem Photobiol 93:912
43. Yun SH, Kwok SJJ (2017) Nat Biomed Eng 1:16
44. Baldwin JE, Crossley MJ, DeBernardis J (1982) Tetrahedron 38:685
45. Alonso CMA, Neves MGPMS, Tomé AC, Silva AMS, Cavaleiro JAS (2005) Tetrahedron 61:11866
46. Faustino MA, Neves MGPMS, Vicente MGH, Silva AMS, Cavaleiro JS (1995) Tetrahedron Lett 36:5977
47. Batalha PN, Gomes ATPC, Forezi LSM, Costa L, de Souza MCBV, Boechat FdCS, Ferreira VF, Almeida A, Neves MGPMS, Cavaleiro JAS (2015) RSC Adv 5:71228
48. Bastos MM, Gomes ATPC, Neves MGPMS, Santos-Filho OA, Boechat N, Cavaleiro JAS (2013) Eur J Org Chem 1485
49. Hashimoto T, Choe Y-K, Nakano H, Hirao K (1999) J Phys Chem A 103:1894
50. Baskin JS, Yu H-Z, Zewail AH (2002) J Phys Chem A 106:9837
51. Durantini J, Otero L, Funes M, Durantini EN, Fungo F, Gervaldo M (2011) Electrochim Acta 56:4126
52. Maximiano RV, Piovesan E, Zílio SC, Machado AEH, de Paula R, Cavaleiro JAS, Borissevitch IE, Ito AS, Gonçalves PJ, Neto NMB (2010) J Photochem Photobiol A 214:115
53. Berlman IB (1971) Handbook of fluorescence spectra of aromatic molecules, 2nd edn. Academic, New York
54. Montalti AC, Prodi L, Gandolfi MT (2006) Handbook of photochemistryn, 3rd edn. Taylor & Francis, Boca Raton
55. Spiller W, Kliesch H, Wöhrle D, Hackbarth S, Röder B, Schnurpfeil G (1998) J Porphyrins Phthalocyanines 2:145
56. Zenkevich E, Sagun E, Knyukshto V, Shulga A, Mironov A, Efremova O, Bonnett R, Songca SP, Kassem M (1996) J Photochem Photobiol B 33:171
57. Armarego WLF, Perrin DD (1996) Purification of laboratory chemicals, 4th edn. Butterworth-Heinemann, Oxford
58. Ermilov EA, Tannert S, Werncke T, Choi MTM, Ng DKP, Röder B (2006) Chem Phys 328:428